ACS APPLIED MATERIALS & INTERFACES

Research Article

www.acsami.org

Electromagnetic Interference Shielding Materials Derived from Gelation of Multiwall Carbon Nanotubes in Polystyrene/Poly(methyl methacrylate) Blends

Rani Rohini and Suryasarathi Bose*

Department of Materials Engineering, Indian Institute of Science, Bangalore 560012, India

ABSTRACT: Blends of polystyrene (PS) and poly(methyl methacrylate) (PMMA) with different surface-functionalized multiwall carbon nanotubes (MWNTs) were prepared by solution blending to design materials with tunable EMI (electromagnetic interference) shielding. Different MWNTs like pristine, amine (~NH_2), and carboxyl acid (~COOH) functionalized were incorporated in the polymer by solution blending. The specific interaction driven localization of MWNTs in the blend during annealing was monitored using contact mode AFM (atomic force microscopy) on thin films. Surface composition of the phase separated blends was further evaluated using X-ray photoelectron spectroscopy (XPS). The localization of MWNTs in a given phase in the bulk was further supported by selective dissolution experiments. Solution-casted PS/PMMA (50/50, wt/wt) blend exhibited a cocontinuous morphology on annealing for 30 min, whereas on longer annealing times it coarsened into matrix-droplet type of morphology. Interestingly, both pristine MWNTs and NH_2-MWNTs resulted in interconnected structures of PMMA in PS matrix upon annealing, whereas COOH-MWNTs were localized in the PMMA droplets. Room-temperature electrical conductivity and electromagnetic shielding effectiveness (SE) were measured in a broad range of frequency. It was observed that both electrical conductivity and SE were strongly contingent on the type of surface functional groups on the MWNTs. The thermal conductivity of the blends was measured with laser flash technique at different temperatures. Interestingly, the SE for blends with pristine and NH_2-MWNTs was >−24 dB at room temperature, which is commercially important, and with very marginal variation in thermal conductivity in the temperature range of 303−343 K. The gelation of MWNTs in the blends resulted in a higher SE than those obtained using the composites.

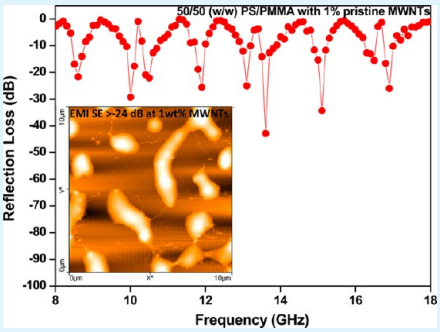

KEYWORDS: *PS/PMMA blends, MWNTs, electrical conductivity, EMI shielding, thermal conductivity*

INTRODUCTION

In view of their exceptional properties like high electrical conductivity,[1] good mechanical strength,[2] and high thermal conductivity,[3] carbon nanotubes (CNTs) have emerged as a potential candidate for numerous applications. In the past decade, polymer-based nanocomposites have been extensively studied and various intriguing properties have been reported. It is now understood that the key to realizing these extraordinary properties lies in their uniform dispersion in the polymer matrix. Broadly, two different strategies, such as covalent and noncovalent functionalization, have been adopted with respect to their uniform dispersion. Recently, a unique strategy of controlling their dispersion has been reported via phase separation in polymer blends.[4] The CNTs migrate to their energetically favored phase during phase separation. This leads to an effective increase in the local concentration of CNTs in a given phase, resulting in the formation of a network like structure at relatively lower fractions. The network like structure of CNTs is often realized in blends that show cocontinuous type of morphologies.[5] Such structures are very interesting from electrical and thermal conductivity points of view, as the overlapping CNTs can tunnel electrons and reduce the mean free path of phonons in striking contrast to random distribution.

Selective localization of conducting particles like CNTs in one of the phases of a cocontinuous blend provides an alternate pathway toward achieving lower percolation threshold in the blends. This has been realized in numerous blend systems, which are highlighted in a recent review.[6] For instance, in PA6/ABS blends, multiwall carbon nanotube (MWNTs) were observed to be selectively localized in the continuous PA6 phase and the percolation threshold was significantly lower than that of PA6/MWNT composites.[7] Co-continuous blends of 60/40 PC/SAN with 2 wt % MWNTs were found to have significantly lower electrical resistivity, which was attributed to selective localization of MWNTs in the PC phase.[8]

Recent increases in electromagnetic (EM) radiations from electronic devices have led to a new kind of problem as electromagnetic pollution. This has led to the design of a new class of materials known as EMI (electromagnetic interference) shielding materials. Metals, being electrically conducting, were used as shielding materials, but suffer from certain disadvantages like corrosion under harsh conditions. In this context, polymer-based composites emerged as a potential alternative to

Received: March 24, 2014
Accepted: July 1, 2014
Published: July 1, 2014

   dx.doi.org/10.1021/am502641h | *ACS Appl. Mater. Interfaces* 2014, 6, 11302−11310

conventional materials because of their ease of fabrication/processing, light weight, and corrosion resistance.[9] Recent studies on polymer/MWNT composites as EMI shielding materials have shown promising results. Increase in EMI shielding effectiveness in the composites can be attributed to the conducting network formed by MWNTs.[10] For instance, PANI-MWNT composite exhibited SE in the range of −27.5 to −39.2 dB in the frequency range of 12−18.0 GHz.[11] PU/SWNTs composites exhibited a SE of ca. 17 dB in the frequency range of 12−18.0 GHz.[12] CNT-PS foams exhibited SE of the order of 19.3 dB at 7 wt % .[13] A high SE of 49 dB was reported at a loading of 15 wt % in epoxy/SWNT composites.[14] Solvent-casted film of MWNT/PMMA composite showed SE of 18 dB at 10 vol % MWNT.[15] Addition of 1 wt % CNT in 10 vol % of carbon nanofiber/PS composite showed a SE of ca. 20.3 dB. Another study on CNT/PMMA composite reported a SE of 27 dB at 40% of CNT loading and a SE of 40 dB at 10 vol % MWNT measured on stacked films.[16] In a recent study, amine-terminated MWNTs were used to enhance the SE in PC/SAN blend.[17]

Thermal conductivity is an important parameter to determine the efficacy of the materials under different temperature conditions. Unlike electrical properties of CNT/polymer composites, thermal properties like conductivity, diffusivity, etc., are less explored and the mechanism is still not well understood.[18] Factors influencing thermal conductivity of CNT/polymer composites have been addressed in a recent review.[19] It has been confirmed experimentally that increase in CNT content and functionalization of CNT improves the thermal transport in the composites.[20,21] However, phonon transfer was observed to be restricted by CNT bundles, which lead to the low thermal conductivity in the composites.[20] Parker et.al.[22] developed a technique known as flash method to measure the thermal diffusivity, heat capacity and thermal conductivity of materials. In this method, the sample coated with camphor was irradiated with high energy light pulse for very short time on the front side and then temperature at the rear face was measured. A plot of temperature versus time gives the thermal diffusivity, whereas heat capacity can be obtained directly from the attached thermocouple. Most often, a laser flash technique is employed to measure the thermal diffusivity for bulk polymers at different temperatures.[23]

It is well-known that PS/PMMA can be casted from a common solvent. The phase separation in PS/PMMA blends has been well studied with respect to annealing time, molecular weight, choice of solvent and the substrate.[24−27] Charge transport properties in conducting-particle-filled PS/PMMA blends was studied in detail in the past.[28,29] In addition, chemical-specific electrical responses in thin PS/PMMA blends was also studied using XPS.[30] Mao et.al. designed conducting 50/50 (w/w) PS/PMMA/GE-ODA composite at low percolation threshold of 0.5 wt % GE-ODA.[31] Although different aspects have been well-characterized for PS/PMMA blends with different conducting particles, the effect of MWNTs on the shield effectiveness did not receive much attention. In this work, different MWNTs, like pristine, NH_2-functionalized, and COOH-functionalized MWNTs, were incorporated in PS/PMMA blends to design materials with tunable EMI SE at lower fractions of MWNTs. The latter is desired as low loading of MWNTs assists in retaining the matrix physical properties and also eases processability of the blends.[32] As different surface-functionalized MWNTs interact differently with the constituents, their localization in a given phase can be tuned. To get a clearer picture of the state of dispersion of MWNTs in 2D (in thin films) and in 3D (in the bulk), topographical AFM and SEM images were recorded. The quality of dispersion of MWNTs in 3D was also supported by selective dissolution experiments. Thermal conductivity and the diffusivity of the composites were studied. The blends with MWNTs showed only a marginal variation in thermal conductivity at higher temperature suggesting an efficient thermal management material with good SE.

EXPERIMENTAL SECTION

Materials. Atactic Polystyrene (M_w 35 000g/mol) was obtained from Sigma-Aldrich and atactic Poly(methyl methacrylate) (PMMA) (Altuglas V825T, M_w 95 000g/mol) was kindly provided by Arkema. Different MWNTs (∼COOH-functionalized (NC3151), ∼NH_2-functionalized (NC3152), and pristine MWNTs (NC7000) were obtained from Nanocyl SA, Belgium. The average diameter of the MWNTs were approximately the same (9.5 nm) as provided by the supplier. However, the length of the pristine MWNTs (1.5 μm) was higher with respect to the functionalized MWNTs (600−700 nm). The concentration of ∼NH_2 and ∼COOH, as determined from XPS, was reported to be 0.5 and 4 wt % respectively. We have also carried out the thermogravimetric analysis of the as received CNTs. The TGA scans (not shown here) reveals that they are stable at the molding temperature (i.e., 200 °C). Solvents of analytical grades were used as received.

Blend Preparation. Solution blending was adopted to prepare the control 50/50 (w/w) PS/PMMA blends and with different MWNTs. The concentration of the MWNTs was fixed at 1 wt % with respect to the total mass of the batch (2g). Tetrahydrofuran (THF) (solubility parameter, δ = 18.6) being a common solvent for both PS (δ = 18.19) and PMMA (δ = 19.65) was selected to prepare the solutions. Both the polymers were dissolved in THF under continuous stirring. MWNTs were separately dispersed in THF and subjected to probe sonication using Heilscher UP 400S for 20 min at 70% amplitude before adding it to the polymer solution. The resultant solution was then shear mixed using Ultra-Turrax T25 for 45 min at 8200 rpm and was then precipitated in excess ethanol which is a nonsolvent for both PS and PMMA.[33] The obtained solid mass was then filtered and was vacuum-dried at 85 °C for 2 days. Neat 50/50 (w/w) PS/PMMA blend was also prepared in the same way. A control sample with 1 wt % NH_2-MWNTs in PMMA were also prepared.

Characterization. Contact mode Atomic Force Microscopy (AFM) was performed using Nanosurf Easy Scan 2 instrument to study the morphology and the state of dispersion of MWNTs on thin films. For AFM, samples of PS/PMMA (0.2% w/v) in THF were spin-coated at 2500 rpm for 2 min onto a silicon wafer. The spin-coated films were then annealed for 30 and 60 min under N_2 atmosphere at 200 °C.

To evaluate the surface composition of the thin films, we carried out X-ray photoelectron spectroscopy (XPS) using Kratos Analytical instrument, which employs a monochromatic Al Kα X-ray source with pass energy of 20 eV. For XPS, spin-coated films of neat PS/PMMA blend was annealed at 200 °C for different annealing times (30 and 60 min).

Scanning electron microscopy (SEM) analysis was performed at an accelerating voltage of 10 kV and spot size of 2 on a FEI Sirion XL30 FEG SEM. Samples were cryo-fractured in liquid nitrogen and PS phase was etched out in cyclohexane for 60 min. SEM was performed on gold-sputtered samples.

For the selective dissolution test, 2 mg of sample was dissolved in 5 mL of cyclohexane (to selectively dissolve PS) and glacial acetic acid (to selectively dissolve PMMA). The vials were then sonicated before digitally recording the state of dispersion of MWNTs in the solution.

Compression molded samples of 10 mm diameter and 1 mm thickness were prepared for electrical conductivity measurements. Room-temperature conductivities were measured using a Novocontrol

(Germany) Alpha-N impedance analyzer in a broad frequency range of 0.1 to 1 × 10^6 Hz.

EMI shielding effectiveness was characterized using an Anritsu MS4642A vector network analyzer (VNA) in the X-band and K_u-band frequencies. The VNA was coupled to a coax setup (Damaskos M 07T). The donut shaped specimens (inner diameter 3 mm, outer diameter 7 mm and thickness of 5 mm) compressed at 200 °C were used and the S parameters (S_{11}, S_{22}, S_{12}, and S_{21}) were recorded in the X-band and in the K_u band using a VNA. The vector network analyzer was calibrated for the full two-port (SOLT, short-open-load and reference through) measurement of reflection and transmission at each port.

For thermal conductivity measurements, samples of 12.6 mm in diameter and 0.75 mm thickness were compression molded at 200 °C. Laser flash technique was employed to measure the thermal conductivity and diffusivity of the blends at different temperatures from 303 to 343 K using a TA Discovery Environmental Module EM-2800. Samples were coated with a very thin layer of graphite to make it opaque to the energy pulse and for uniform spreading of energy pulse through the sample or to improve emissivity. Experiments were performed in Ar atmosphere inside the chamber with liquid-N_2-cooled IR detector placed beneath the sample holder. The thermal conductivity can be obtained as the product of density of the sample, measured thermal diffusivity, and heat capacity.

RESULT AND DISCUSSION

Selective Localization of MWNTs and Surface Composition of Thin Films of PS/PMMA Blends. Selective localization of MWNTs can be predicted, a priori, from classical thermodynamics. By knowing the surface free energy of the entities and their dependence on temperature, the wetting coefficient can be estimated using Young's equation given by,[34]

$$\omega_{AB} = \frac{(\gamma_{p-B} - \gamma_{p-A})}{(\gamma_{AB})} \quad (1)$$

where p, A, and B indicate MWNTs, PS, and PMMA, respectively. γ_{AB}, $\gamma_{p\text{-}A}$, and $\gamma_{p\text{-}B}$ are the interfacial tensions between PS/PMMA, PS/MWNTs, and PMMA/MWNTs, respectively. For $\omega_{AB} > 1$, MWNTs would prefer phase A (i.e., PS) and for $\omega_{AB} < -1$, MWNT would prefer B (i.e., PMMA). For $-1 < \omega_{AB} < 1$, MWNTs would prefer to localize at the interface.

The interfacial tension between the entities can be evaluated using Owens−Wendt−Rebel−Kaelble (OWRK) and Wu's equation.[35] OWRK equation is often employed for nonpolar/polar and Wu's equation for nonpolar/nonpolar systems. In this study, OWRK equation has been used to calculate the interfacial tension between PS and PMMA

$$\gamma_{12} = \gamma_1 + \gamma_2 - 2\sqrt{\gamma_1^d \gamma_2^d} - 2\sqrt{\gamma_1^p \gamma_2^p} \quad (2)$$

γ^d and γ^p are the dispersive and the polar component of the surface energy. Table 1 lists the surface free energy of PS, PMMA and MWNT at 200 °C. From eq 1, ω_{AB} is estimated to be 3.25, which suggests that MWNTs prefer to localize in the PMMA phase of the blends.

Spin-coated samples were annealed for different time scales to probe the microstructure and the localization of MWNTs in the blends. It is envisaged that different surface-functionalized MWNTs would interact differently with the components resulting in differences in the state of dispersion. To assess the state of dispersion of MWNTs in 2D (in thin films) and in 3D (in the bulk), we adopted different strategies. Blends with MWNTs were spin coated and the films were annealed for different time scales. To assess the dispersion state in 3D, we dissolved bulk samples in respective solvents to completely remove the phases. For instance, known amount of samples was dissolved in cyclohexane to completely remove the PS phase from the blends. Alternatively, blend samples were dissolved in glacial acetic acid to completely remove the PMMA phase.

Table 1. Surface Free Energies of PS and PMMA at 200 °C

	surface free energy (mN/m)		
	γ	γ^d	γ^p
PS	27.74	21.64	6.1
PMMA	27.42	15.92	11.5
NH_2-MWNT and COOH-MWNTs[41]	45.3	18.4	28.9
MWNTs[41]	27.8	17.6	10.2

Before evaluating the state of dispersion of MWNTs in thin films, it is important to know the surface composition of the blends especially, when topography is studied using an AFM. In this mode, the AFM tip differentiates the constituents based on the surface roughness. The stiffer component appears brighter in the topographical AFM micrographs. In order to further confirm the phases, XPS scans were recorded on the annealed samples which is an efficient tool to assess the surface composition in biphasic blends. Figure 1 shows the topographical image of 50/50 (w/w) PS/PMMA blend, which was annealed for 30 min. The inset of Figure 1 shows the corresponding XPS scan, typically from the top 10 nm. Interestingly, the XPS scans reveal that the elevated regions which also appear brighter in the topographical images correspond to the PMMA phase. This is manifested from the presence of C_{1s} peak in the XPS scans. The binding energy corresponding to −C−C−/−C−H− (285.0); β-shift C (285.9); −O−C− (286.7) and −O−C═O (289.1 eV) in PMMA is well evident in the deconvoluted spectra.[36] Moreover, the absence of "shake-up" peak corresponding to $\pi \rightarrow \pi^*$ of PS further confirms that the surface is enriched with PMMA. Hence, the brighter regions in the topographical AFM images correspond to the PMMA phase.

As discussed, different surface functional groups on the MWNTs can interact differently with the constituents. To get more insight in the state of dispersion of MWNTs in the blends, we recorded topographical images on thin films after annealing for 60 min. Figure 2 shows the 2D AFM topographical images of the blends with different MWNTs. The corresponding vials in which the composite samples were dissolved in cyclohexane (to dissolve completely the PS phase) and glacial acetic acid (to dissolve completely the PMMA phase) are also included here. By comparing this way the selective localization of MWNTs in both 2D (in thin films) and 3D (in the bulk) can be assessed systematically. As observed from the AFM topographical images, pristine MWNTs and NH_2-MWNTs are observed to bridge the PMMA phases in the blends. However, in the bulk, they appear to be localized mainly in the PMMA phase but partially in the PS phase as well. The latter is supported by the fact that the solution corresponding to the PS appears to be gray (see inset of Figure 2a). Similar observations are noted in the case of blends with NH_2-MWNTs as well. Interestingly, the topographical AFM images of the blends with COOH-MWNTs, reveal discrete domains of PMMA in PS matrix. It suggests that COOH-MWNTs are strictly localized in the PMMA phase of the blend because of the specific interaction between the ∼COOH group on the surface of MWNTs and −O−C═O of PMMA.[37] This phenomenon is also supported by the state of dispersion in

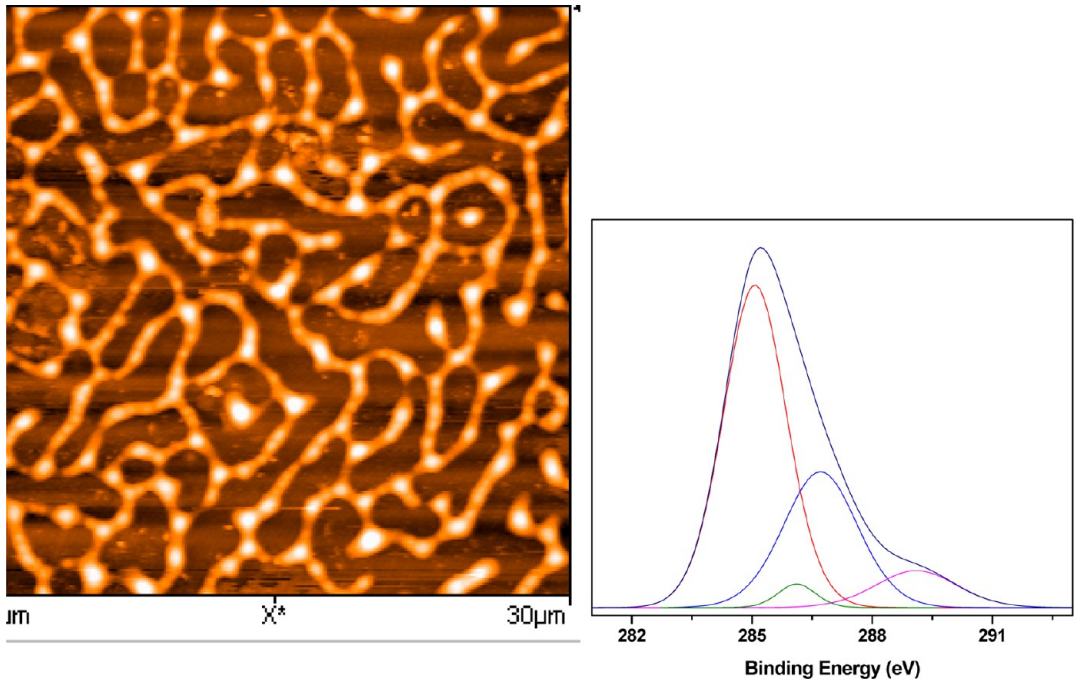

Figure 1. AFM 2D topography of 50/50 (w/w) PS/PMMA blends. Inset shows the XPS spectra corresponding to C_{1s}.

3D, where the vial corresponding to glacial acetic acid is completely dark while the other is blank. It can be argued that the interconnected PMMA phases facilitated by pristine MWNTs can be explained based on the fact that the characteristic length scales of pristine MWNTs are larger than the phase dimensions. Interestingly enough, the blends with NH_2-MWNTs also revealed interconnected PMMA domains in PS matrix; however, these MWNTs are shorter by a factor of 2. To get a clearer picture, we annealed the blends at different time scales. One set of blends was annealed for 30 min and the other for 60 min; they are discussed in the next section.

Effect of Annealing Time on the Morphology of PS/PMMA Blends: Influence of MWNTs. Figure 3 shows the AFM topographical images of control 50/50 (w/w) PS/PMMA blend and with different MWNTs under different annealing times. The stack of images on the extreme left represent the morphologies of the blends before annealing; the center column represents after 30 min of annealing and the stack of images in the extreme right displays after 60 min of annealing. It is interesting to note that neat PS/PMMA blends exhibit matrix-droplet type of morphology before annealing and the interfacial driven coarsening facilitates cocontinuous morphologies at intermediate annealing times (30 min). As this transient morphology is not at equilibrium, it coarsens further to matrix-droplet type in order to minimize the surface free energy. These phenomenal transitions are quite different in the case of MWNTs, especially with different types of MWNTs. For instance, in the case of pristine MWNTs, a well-defined cocontinuous morphology is observed initially that coarsened into a sea-island type of morphology in the late stages of coarsening. Intriguingly, in the late stage, interconnected PMMA domains bridged by MWNTs are noted. Such observations were earlier reported in the case of PαMSAN/PMMA blends where MWNTs were observed to connect the droplets resulting in an irregular structure.[20] Similar observations were noted in the case of NH_2-MWNTs except for the fact that the domain sizes were much smaller. The mechanism of coarsening in PS/PMMA blends has been well- documented.[27] It is now understood that both pristine MWNTs and NH_2-MWNTs promote interconnected PMMA domains during interfacial driven coarsening in the late stages of annealing. Interestingly, the blends with COOH-MWNTs also led to smaller domain size though, they were selectively localized in the PMMA domains. The gelation of MWNTs in a given phase of biphasic blends can result in intriguing electrical conductivity in the blends and is discussed in the next section.

Gelation of MWNTs in PMMA: High Electrical Conductivity and EMI Shielding. Figure 4 displays the SEM images of the blends with different MWNTs. Higher-resolution images are also shown as inset here. The PS phase was etched using cyclohexane to improve the contrast between the phases. It is well observed, especially from the high resolution images, that MWNTs are mostly localized in the PMMA phase of the blends in the case of both pristine MWNTs and NH_2-MWNTs and are also observed to bridge the PMMA domains. This observation is in close agreement with AFM. The interesting observation that draws our attention here is that the MWNTs form an interconnected network in the PMMA phase of the blends which is very evident from the high resolution SEM images. From the cryofractured and etched samples, dense matlike structures of MWNTs bridging the phases are well evident. But no such features were observed in the case of COOH-MWNTs. Such gelation of MWNTs can result in very high electrical conductivity in the blends and is discussed in the next section.

Figure 5 shows the AC electrical conductivity as a function of frequency for PS/PMMA blends and with different MWNTs at room temperature. Neat PS/PMMA blends displayed a behavior of a typical insulator where conductivity increases rapidly with increase in frequency. Blends with pristine MWNTs and NH_2-MWNTs showed conductivity with significantly higher electrical conductivity with respect to the neat blends of the order of 10^{-5} S/cm. This high electrical

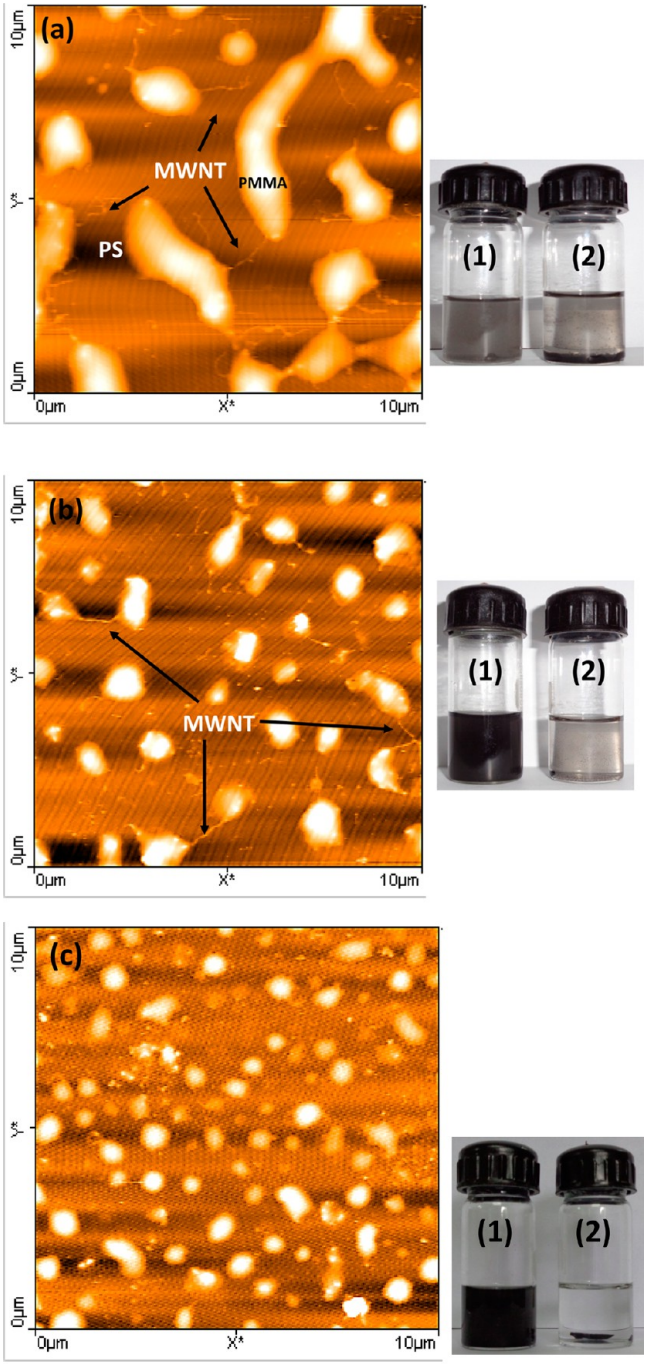

Figure 2. AFM 2D topographical images of PS/PMMA blends with (a) pristine MWNTs; (b) NH2-MWNTs; (c) COOH-MWNTs. Insets show the corresponding vials where PS was completely dissolved using cyclohexane (vial 1) and PMMA by glacial acetic acid (vial 2). The dark solution represent MWNTs in the respective phases.

conductivity can be attributed to gelation of MWNTs in the PMMA phase of the blends. Such interconnected network structure assists electrons in tunneling, resulting in a very high electrical conductivity in the composites. In the case of blends with COOH-MWNTs, the increase in conductivity was only marginal possibly because of a lower degree of interconnected MWNTs. In addition to this, coulomb traps in COOH-MWNTs can also result in lower electrical conductivity in the blends.[4]

It is worth noting that high electrical conductivity in PS/PMMA blends could be achieved with only 1 wt % of MWNTs. The higher bulk electrical conductivity in pristine MWNTs and NH_2-MWNTs accords well with the observation of interconnected network of MWNTs in 2D (in thin films) and in 3D (bulk). Interestingly, PMMA with pristine-MWNTs composites showed one order lower electrical conductivity with respect to PMMA/PS blends with 1 wt % NH_2-MWNTs. Such materials can further be explored as potential materials to attenuate the EM waves. EMI shielding effectiveness is the quantification of the total attenuated EM waves.[38] The shielding effectiveness (SE) is defined as the ratio of the power of incident EM waves to the power of transmitted EM waves and is expressed as eq 3, where I and T are the power of the incident and the transmitted waves, and expressed in decibels (dB). The total EMI SE comprises of reflection, absorption and multiple reflections of EM waves.[10] It depends on the shielding material thickness and applied frequency range of EM waves.[38]

$$SE_T = 10\log(I/T) \tag{3}$$

$$SE_T = 10\log\frac{1}{|S_{21}|2} \tag{4}$$

$$RL(\mathrm{dB}) = 20\log\frac{|Z_{in} - 1|}{|Z_{in} + 1|} \tag{5}$$

$$Z_{in} = j\sqrt{\frac{\mu_r}{\varepsilon_r}}\tan\left(\frac{2\pi fd\sqrt{\mu_r\varepsilon_r}}{c}\right) \tag{6}$$

The VNA, coax set up, and other elements are pictorially depicted in images a and b in Figure 6. Figure 6c illustrates the SE of PS/PMMA blends with different MWNTs. Total EMI shielding effectiveness was measured using eq 4.[17] Reflection loss (RL) was calculated from eqs 5 and 6.[39] Interestingly, the blends with pristine MWNTs and NH_2-MWNTs display a very high SE, of the order of −24.1 and −24.6 dB, respectively. It is now understood that interconnected network like structure of MWNTs is an essential criteria toward enhanced SE. Another observation draws our attention here. The high SE in the blends in the presence of pristine MWNTs and NH_2-MWNTs is in the frequency range of 12−16 GHz, which essentially suggests that these materials can shield both in the X-band frequency (8−12 GHz) and as well as in the microwave frequency regime (12−16 GHz). The latter is interesting from military radar and other high end application point of view. It is envisaged that high SE is a direct consequence of high electrical conductivity in the composites.[40] The blends with COOH-MWNTs showed a rather low SE of −9.7 dB at 1 wt %. Another observation which is of interest is that PMMA/NH_2-MWNTs composites showed a SE of −18 dB, which is lower than the blends at a given fraction of MWNTs. Hence, this study clearly demonstrates that gelation of MWNTs in a given phase of binary blends can be used as an efficient tool to design materials with high SE.

For further discussion on the attenuation of microwave frequencies, we considered only blends with NH_2-MWNTs and pristine MWNTs as they showed ca. 99.8% attenuation. Interestingly, blends with NH_2-MWNTs showed the highest RL value of −43.06 dB at 9.9 GHz, whereas blends with pristine MWNTs showed RL of −42.9 dB at 13.6 GHz (Figure 6d). This essentially indicates that the absorbing peak is

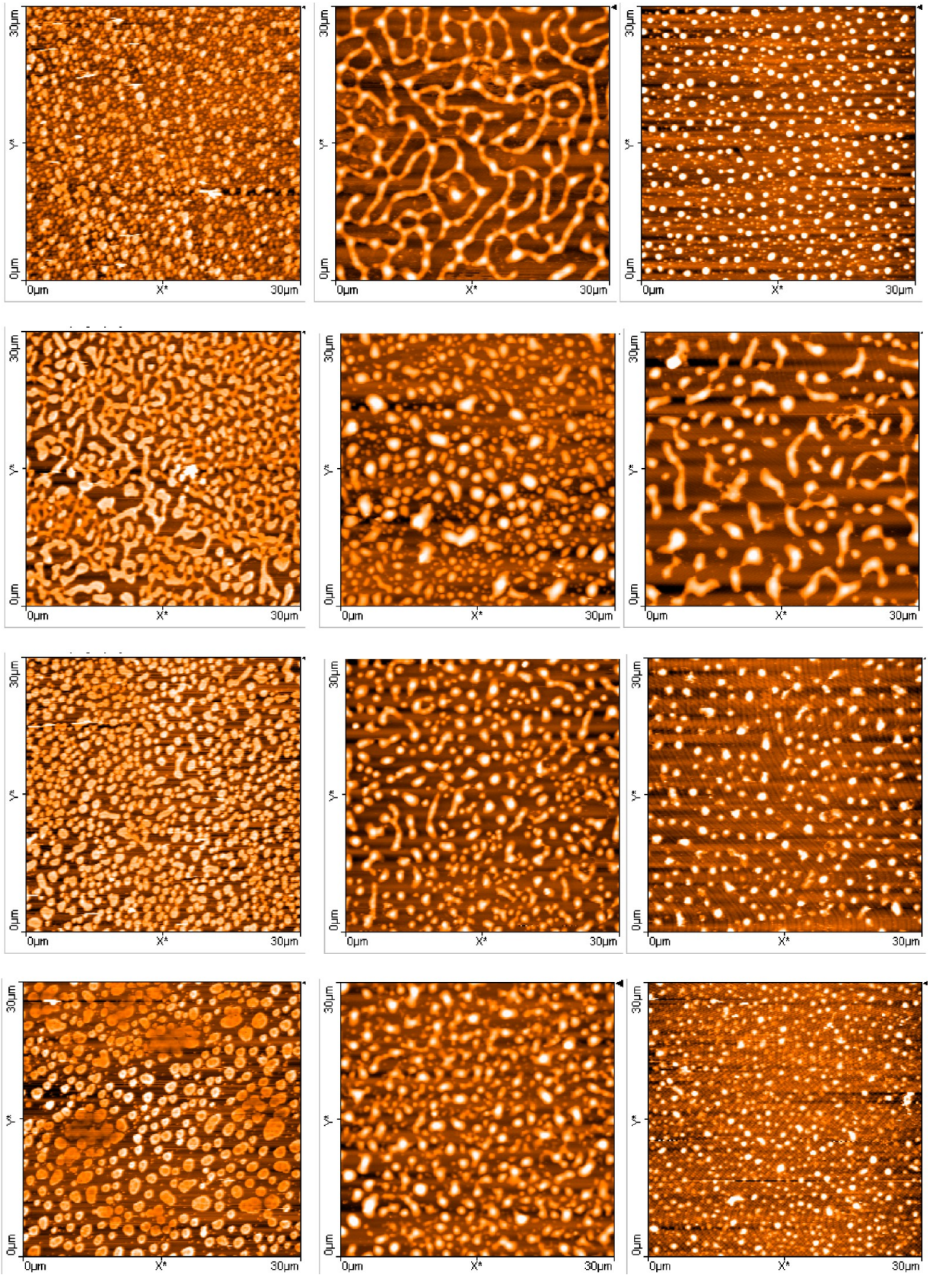

Figure 3. AFM 2D topographical images of neat blends (first row), blends with pristine MWNTs (second row), NH_2-MWNTs (third row), and COOH-MWNTs (fourth row) under different conditions. The left column represents stack of images before annealing; the middle column represents after annealing for 30 min; and the right column represents images captured after annealing for 60 min.

dx.doi.org/10.1021/am502641h | *ACS Appl. Mater. Interfaces* 2014, 6, 11302−11310

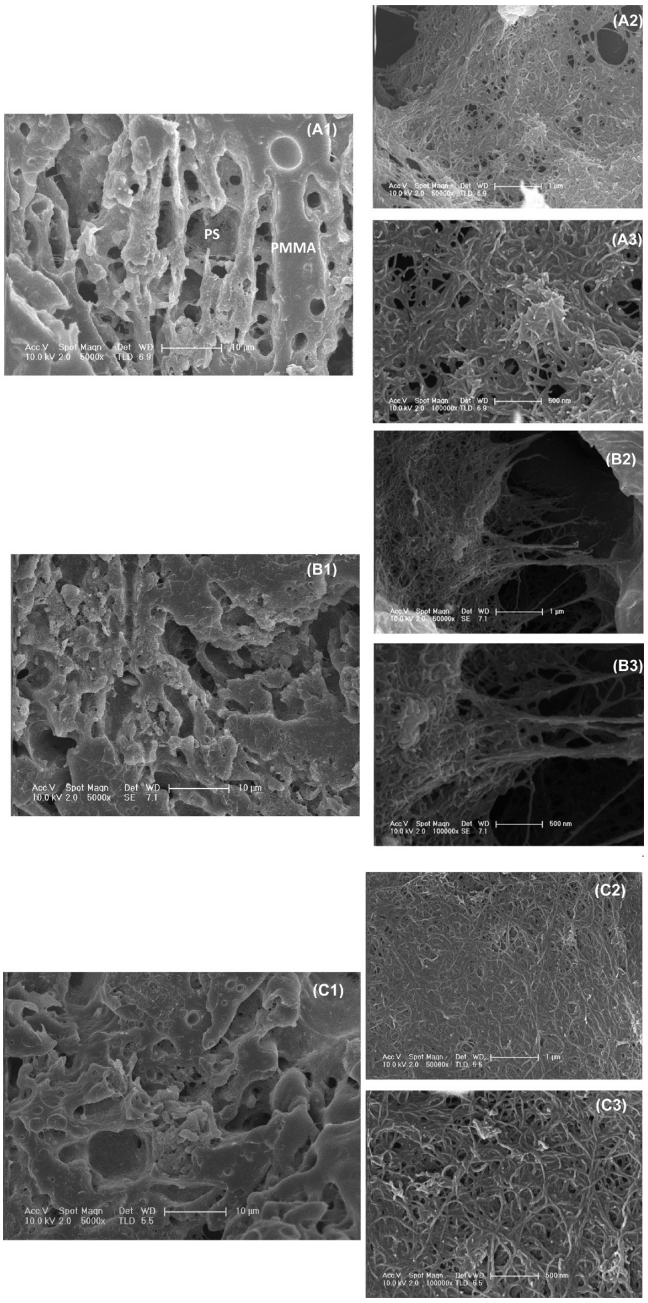

Figure 4. SEM micrographs of PS/PMMA blend with (A1) COOH-MWNTs, (B1) NH_2-MWNTs, and (C1) pristine MWNTs. The inset shows higher resolution images of the corresponding blends.

maximum at 9.9 GHz for NH_2-MWNTs and 13.6 GHz for pristine MWNTs.

Gelation of MWNTs in PS/PMMA Blends: Effect on Thermal Conductivity. From the above observations, it can be concluded that the composites under investigation can be explored as EMI shielding materials. It is well understood that heat is an unavoidable byproduct in operating electronics which if not taken care of can result in decreased reliability. The current flowing through the active and passive components result in power dissipation and increased temperatures. Hence, a good electronic packaging material, apart from shielding external EM waves, should sustain the rise in temperature without any structural distortion. Hence, probing the thermal conductivity and the diffusivity in these blends is very essential.

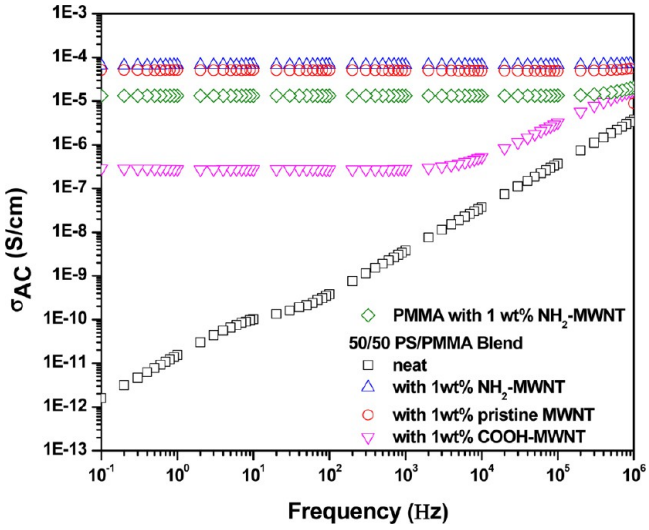

Figure 5. Room-emperature AC conductivity as a function of frequency for neat blends and with different MWNTs, and 1 wt % NH_2-MWNT/PMMA composite.

To accomplish this, thermal conductivity and diffusivity at different temperatures (313−333 K) was measured on 50/50 (w/w) PS/PMMA blends with different MWNTs (see Figure 7). It is well understood that aligned MWNT exhibit efficient thermal conductive path for phonons and is very different from the percolate network like structure of CNTs required for high electrical conductivity. Intriguingly, the blends with pristine, and NH_2-MWNTs showed no appreciable change in the thermal conductivity in the temperature range of 313−333 K which essentially suggest that these materials can withstand these temperature without sacrificing the structural integrity. This observation is also manifested from the thermal diffusivity values (see inset of Figure 7). A higher thermal diffusivity in the blends with pristine MWNTs and NH_2-MWNTs with respect to COOH-MWNTs further supports the interconnected network like structure of MWNTs in the PMMA phase. Thermal resistance arises from phonon scattering and hence, the interconnected network of MWNTs in PS/PMMA blends in the presence of pristine, and NH_2-MWNTs facilitate phonon transfer and can be used as a thermal management with good SE material.

CONCLUSIONS

In this work, different MWNTs were incorporated in PS/PMMA blends to design materials with high EMI SE. The state of dispersion of MWNTs in 2D (spin-coated thin films) and in the bulk (3D) was assessed using AFM and selective dissolution, respectively. Higher electrical conductivity and significantly higher EMI SE in the blends is attributed to the gelation of MWNTs in the PMMA phase of the blends. Further, interconnected PMMA domains bridged by MWNTs were observed in the annealed blends. Thermal conductivity and the diffusivity were also observed to be higher in the case of pristine, and NH_2-MWNTs in striking contrast to COOH-MWNTs. Moreover, the thermal conductivity more or less remains unaltered in the temperature range of 313−333 K. It is believed that interconnected network of MWNTs in PS/PMMA blends facilitated by pristine, and NH_2-MWNTs results in efficient phonon transfer and can be used as a thermal management material with good SE.

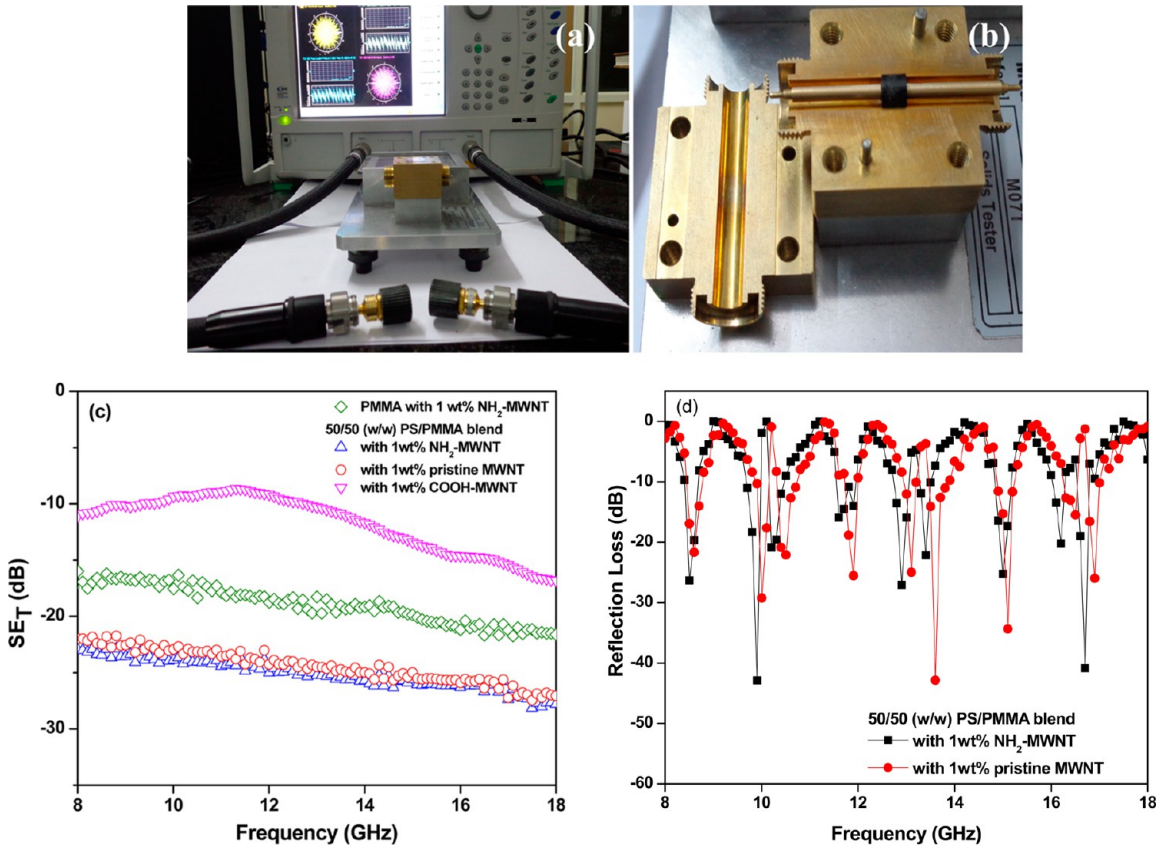

Figure 6. (a) VNA setup; (b) coax setup; (c) total shielding effectiveness as a function of frequency for blends with different MWNTs and 1 wt % NH_2-MWNT/PMMA composite at room temperature; and (d) reflection loss as a function of frequency for blends with pristine and NH_2-MWNTs.

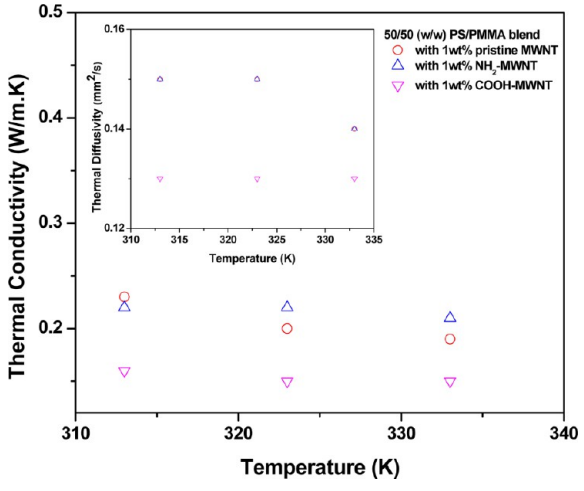

Figure 7. Thermal conductivity as a function temperature for PS/PMMA blends with different MWNTs. Inset shows the thermal diffusivity at the corresponding temperatures.

AUTHOR INFORMATION

Corresponding Author

*E-mail: sbose@materials.iisc.ernet.in. Tel: +91-80-2293 3407.

Notes

The authors declare no competing financial interest.

ACKNOWLEDGMENTS

The authors acknowledge financial support from DST and CSIR, AFMM (IISc) for SEM facility and Mr. Olu Emmanuel Femi for his assistance with thermal conductivity measurements.

REFERENCES

(1) Ebbesen, T.; Lezec, H.; Hiura, H.; Bennett, J.; Ghaemi, H.; Thio, T. Electrical Conductivity of Individual Carbon Nanotubes. *Nature* **1996**, *382*, 54−56.

(2) Treacy, M.; Ebbesen, T.; Gibson, J. Exceptionally High Young's Modulus Observed for Individual Carbon Nanotubes. *Nature* **1996**, *381*, 678−680.

(3) Fujii, M.; Zhang, X.; Xie, H.; Ago, H.; Takahashi, K.; Ikuta, T.; Abe, H.; Shimizu, T. Measuring the Thermal Conductivity of a Single Carbon Nanotube. *Phys. Rev. Lett.* **2005**, *95*, 065502−01- 065502−04.

(4) Özdilek, C.; Bose, S.; Leys, J.; Seo, J. W.; Wübbenhorst, M.; Moldenaers, P. Thermally Induced Phase Separation in PαMSAN/PMMA Blends in presence of Functionalized Multiwall Carbon Nanotubes: Rheology, Morphology and Electrical Conductivity. *Polymer* **2011**, *52*, 4480−4489.

(5) Bose, S.; Bhattacharyya, A. R.; Khare, R. A.; Kulkarni, A. R.; Pötschke, P. Specific Interactions and Reactive Coupling Induced Dispersion of Multiwall Carbon Nanotubes in Co continuous Polyamide6/Ionomer blends. *Macromol. Symp.* **2008**, *263*, 11−20.

(6) Brigandi, P. J.; Cogen, J. M.; Pearson, R. A. Electrically Conductive Multiphase Polymer Blend Carbon-based Composites. *Polym. Eng. Sci.* **2014**, *54*, 1−16.

(7) Meincke, O.; Kaempfer, D.; Weickmann, H.; Friedrich, C.; Vathauer, M.; Warth, H. Mechanical Properties and Electrical Conductivity of Carbon-Nanotube filled Polyamide-6 and its Blends with Acrylonitrile/Butadiene/Styrene. *Polymer* **2004**, *45*, 739−748.

(8) Göldel, A.; Kasaliwal, G.; Pötschke, P. Selective Localization and Migration of Multiwalled Carbon Nanotubes in Blends of Polycarbonate and Poly (styrene-acrylonitrile). *Macromol. Rapid Commun.* **2009**, *30*, 423−429.

(9) Huang, C. Y.; Pai, J. F. Studies on Processing Parameters and Thermal Stability of ENCF/ABS composites for EMI Shielding. *J. Appl. Polym. Sci.* **1997**, *63*, 115−123.
(10) Maiti, S.; Suin, S.; Shrivastava, N. K.; Khatua, B. A Strategy to Achieve High Electromagnetic Interference Shielding and Ultra Low Percolation in Multiwall Carbon Nanotube−Polycarbonate Composites through Selective Localization of Carbon Nanotubes. *RSC Adv.* **2014**, *4*, 7979−7990.
(11) Saini, P.; Choudhary, V.; Singh, B.; Mathur, R.; Dhawan, S. Polyaniline−MWCNT nanocomposites for Microwave Absorption and EMI Shielding. *Mater. Chem. Phys.* **2009**, *113*, 919−926.
(12) Liu, Z.; Bai, G.; Huang, Y.; Ma, Y.; Du, F.; Li, F.; Guo, T.; Chen, Y. Reflection and Absorption Contributions to the Electromagnetic Interference Shielding of Single-walled Carbon Nanotube/Polyurethane composites. *Carbon* **2007**, *45*, 821−827.
(13) Yang, Y.; Gupta, M. C.; Dudley, K. L.; Lawrence, R. W. Novel Carbon Nanotube-Polystyrene Foam Composites for Electromagnetic Interference Shielding. *Nano Lett.* **2005**, *5*, 2131−2134.
(14) Li, N.; Huang, Y.; Du, F.; He, X.; Lin, X.; Gao, H.; Ma, Y.; Li, F.; Chen, Y.; Eklund, P. C. Electromagnetic Interference Shielding of Single-walled Carbon Nanotube Epoxy composites. *Nano Lett.* **2006**, *6*, 1141−1145.
(15) Mathur, R.; Pande, S.; Singh, B.; Dhami, T. Electrical and Mechanical Properties of Multi-Walled Carbon Nanotubes Reinforced PMMA and PS Composites. *Polym. Compos.* **2008**, *29*, 717−727.
(16) Pande, S.; Singh, B.; Mathur, R.; Dhami, T.; Saini, P.; Dhawan, S. Improved Electromagnetic Interference Shielding Properties of MWCNT−PMMA Composites using Layered Structures. *Nanoscale Res. Lett.* **2009**, *4*, 327−334.
(17) Pawar, S. P.; Pattabhi, K.; Bose, S. Assessing The Critical Concentration Of NH_2 Terminal Groups on the Surface of MWNTs Towards Chain Scission of PC in PC/SAN Blends: Effect on Dispersion, Electrical Conductivity and EMI Shielding. *RSC Adv.* **2014**, *4*, 18842−18852.
(18) Gojny, F. H.; Wichmann, M. H.; Fiedler, B.; Kinloch, I. A.; Bauhofer, W.; Windle, A. H.; Schulte, K. Evaluation and Identification of Electrical and Thermal Conduction Mechanisms in Carbon Nanotube/Epoxy Composites. *Polymer* **2006**, *47*, 2036−2045.
(19) Han, Z.; Fina, A. Thermal Conductivity of Carbon Nanotubes and their Polymer Nanocomposites: a Review. *Prog. Polym. Sci.* **2011**, *36*, 914−944.
(20) Yang, S. Y.; Ma, C.C. M.; Teng, C. C.; Huang, Y. W.; Liao, S. H.; Huang, Y. L.; Tien, H. W.; Lee, T. M.; Chiou, K. C. Effect of Functionalized Carbon Nanotubes on the Thermal Conductivity of Epoxy composites. *Carbon* **2010**, *48*, 592−603.
(21) Song, Y. S.; Youn, J. R. Evaluation of Effective Thermal Conductivity for Carbon Nanotube/Polymer Composites using Control Volume Finite Element Method. *Carbon* **2006**, *44*, 710−717.
(22) Parker, W.; Jenkins, R.; Butler, C.; Abbott, G. Flash Method of Determining Thermal Diffusivity, Heat Capacity, and Thermal Conductivity. *J. Appl. Phys.* **1961**, *32*, 1679−1684.
(23) Nunes dos Santos, W.; Mummery, P.; Wallwork, A. Thermal Diffusivity of Polymers by the Laser Flash Technique. *Polym. Test.* **2005**, *24*, 628−634.
(24) Morin, C.; Ikeura-Sekiguchi, H.; Tyliszczak, T.; Cornelius, R.; Brash, J.; Hitchcock, A.; Scholl, A.; Nolting, F.; Appel, G.; Winesett, D. X-ray Spectromicroscopy of Immiscible Polymer Blends: Polystyrene−Poly (methyl methacrylate). *J. Electron Spectrosc. Relat. Phenom.* **2001**, *121*, 203−224.
(25) Li, X.; Han, Y.; An, L. Annealing Effects on the Surface Morphologies of Thin PS/PMMA Blend Films with Different Film Thickness. *Appl. Surf. Sci.* **2004**, *230*, 115−124.
(26) Ugur, S.; Pekcan, O. Effects of Annealing on Morphology of Polymer/Polymer (PS/PMMA) blend; a Fluorescence Study. *J. Appl. Polym. Sci.* **2006**, *100*, 2104−2110.
(27) Cui, L.; Ding, Y.; Li, X.; Wang, Z.; Han, Y. Solvent and Polymer Concentration Effects on the Surface Morphology Evolution of Immiscible Polystyrene/Poly (methyl methacrylate) blends. *Thin Solid Films* **2006**, *515*, 2038−2048.
(28) Calberg, C.; Blacher, S.; Gubbels, F.; Brouers, F.; Deltour, R.; Jérôme, R. Electrical and Dielectric Properties of Carbon Black filled Co-continuous Two-phase Polymer blends. *J. Phys. D: Appl. Phys.* **1999**, *32*, 1517.
(29) Lee, M. S.; Ha, M. G.; Ko, H. J.; Yang, K. S.; Lee, W. J.; Park, M. Morphology and Electrical Conductivity of PS/PMMA/SMMA Blends Filled with Carbon Black. *Fibers and Polym.* **2000**, *1*, 32−36.
(30) Sezen, H.; Ertas, G.; Dâna, A.; Suzer, S. Charging/Discharging of thin PS/PMMA films as Probed by Dynamic X-ray Photoelectron Spectroscopy. *Macromolecules* **2007**, *40*, 4109−4112.
(31) Mao, C.; Zhu, Y.; Jiang, W. Design of Electrical Conductive Composites: Tuning the Morphology to Improve the Electrical Properties of Graphene Filled Immiscible Polymer Blends. *ACS Appl. Mater. Interfaces* **2012**, *4*, 5281−5286.
(32) Ramasubramaniam, R.; Chen, J.; Liu, H. Homogeneous Carbon Nanotube/Polymer Composites for Electrical Applications. *Appl. Phys. Lett.* **2003**, *83*, 2928−2930.
(33) Xavier, P.; Bose, S. Multiwalled-Carbon-Nanotube-Induced Miscibility in Near-Critical PS/PVME Blends: Assessment Through Concentration Fluctuations and Segmental Relaxation. *J. Phys. Chem. B* **2013**, *117*, 8633−8646.
(34) Sumita, M.; Sakata, K.; Asai, S.; Miyasaka, K.; Nakagawa, H. Dispersion of Fillers and the Electrical Conductivity of Polymer Blends Filled with Carbon Black. *Polym. Bull.* **1991**, *25*, 265−271.
(35) Mural, P. K. S.; Madras, G.; Bose, S. Positive Temperature Coefficient and Structural Relaxations in Selectively Localized MWNTs in PE/PEO Blends. *RSC Adv.* **2014**, *4*, 4943−4954.
(36) Ton-That, C.; Shard, A.; Teare, D.; Bradley, R. XPS and AFM Surface Studies of Solvent-cast PS/PMMA blends. *Polymer* **2001**, *42*, 1121−1129.
(37) McClory, C.; McNally, T.; Baxendale, M.; Pötschke, P.; Blau, W.; Ruether, M. Electrical and Rheological Percolation of PMMA/MWCNT Nanocomposites as a Function of CNT Geometry and Functionality. *Eur. Polym. J.* **2010**, *46*, 854−868.
(38) Huang, Y. L.; Yuen, S.-.; Ma, C.-. M.; Chuang, C.-.; Yu, K.; Teng, C. C.; Tien, H. W.; Chiu, Y. C.; Wu, S. Y.; Liao, S. H. Morphological, Electrical, Electromagnetic Interference Shielding, and Tribological Properties of Functionalized Multi-walled Carbon Nanotube/Poly methyl methacrylate (PMMA) composites. *Compos. Sci. Technol.* **2009**, *69*, 1991−1996.
(39) Cao, M.-S.; Song, W.-L.; Hou, Z.-L.; Wen, B.; Yuan, J. The Effects of Temperature and Frequency on the Dielectric Properties, Electromagnetic Interference Shielding and Microwave-Absorption of Short Carbon Fiber/Silica Composites. *Carbon* **2010**, *48*, 788−796.
(40) Xiang, C.; Pan, Y.; Guo, J. Electromagnetic Interference Shielding Effectiveness of Multiwalled Carbon Nanotube Reinforced Fused Silica composites. *Ceram. Int.* **2007**, *33*, 1293−1297.
(41) Nuriel, S.; Liu, L.; Barber, A.; Wagner, H. Direct Measurement of Multiwall Nanotube Surface Tension. *Chem. Phys. Lett.* **2005**, *404*, 263−266.